The emergence of latent infection in the early evolution of *Mycobacterium tuberculosis*

Supplementary material

Rebecca H. Chisholm[*†] **and Mark M. Tanaka**[*†]

[*]School of Biotechnology and Biomolecular Sciences, University of New South Wales, Sydney 2052, Australia
[†] Evolution & Ecology Research Centre, University of New South Wales, Sydney 2052, Australia

This supplementary material includes Figures S1–S3, Table S1 and we address the following matters.

A. We outline the details of the computational algorithm.

B. We provide an analysis of the continuum limit of the discrete model that we have simulated, showing how the integrodifferential equation model emerges under appropriate approximations.

C. We derive a mathematical expression for the basic reproductive number R_0

D. We outline the invasion analysis of our model which shows that a strain with the highest R_0 drives all other strains to extinction

E. We analyse the topography of R_0 which allows us to predict the outcome of an evolution experiment

F. We discuss our assumptions regarding how the fitness landscape changed due to evolution of the interaction between *M. tuberculosis* and human hosts

G. We outline the technical details of our simulations which were performed in MATLAB

H. Caption for the electronic supplementary material, movie S1

A. Computational model of M. tuberculosis evolution

The computational algorithm is shown schematically in Figure. S1. Individual agents in the agent-based computational model represent a human host infected by a particular strain of *M. tuberculosis*. Infections are classified as either active or latent, and are further characterised by two characters $x \in [0, 1]$ and $y \in [0, 1]$ that represent the infecting strain's respective level of potential latency and the probability that the infecting strain enters a latent state upon infection.

Evolution of the system is simulated in discrete time (with time-step length τ). During each time step, each agent undergoes a random walk in a discretised two-dimensional phenotype space (with lattice spacing Δ), followed by stochastic switching between classes of infection, and then the birth and death of agents with phenotype-dependent death rates and phenotype- and density-dependent transmission rates. The random walk captures stochastic variation in an infecting *M. tuberculosis* strain's phenotype due to genetic mutations or epimutations, while the birth and death of agents models the introduction of new infections (due to transmission events) and the loss of infections (due to recovery and host death) from the system.

In the details that follow, i, j and n are integers (where i and j are trait position coordinates such that $x = i\Delta$ and $y = j\Delta$, and n is a discrete time point), the random variables $L_n(i, j)$ and $A_n(i, j)$ are the respective number of latent agents and active agents of phenotype $(x, y) = (i\Delta, j\Delta)$

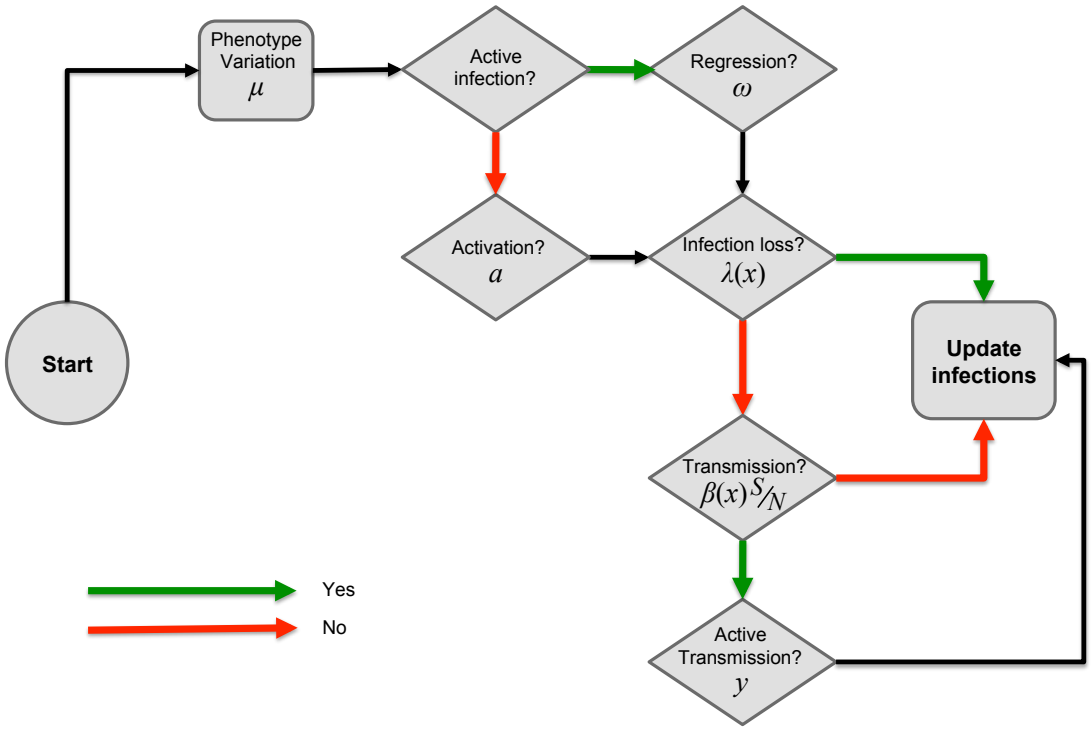

Figure S1: Flow chart describing the decision process for each infection in the agent-based model, with diamonds representing decisions, green arrows meaning the conditions are satisfied, and red meaning the condition is not met. First, infecting strains undergo stochastic incremental changes in phenotype at rate μ. Second, active infections can regress to latency at rate ω or latent infections can reactivate at a rate a. Third, infections are lost if the host dies or recovers from the infection. This occurs at a rate $\lambda(x) = \gamma(x) + \theta(x)$ for latent strains and $\lambda(0) = \gamma(0) + \theta(0)$ for active strains. Finally, current infections can cause new infections, with the rate of transmission of a latent infecting strain $\beta(x)S_n/N$ being dependent on its potential degree of latency x as well as the fraction of susceptible hosts S_n/N, while the rate of transmission of an active infecting strain is $\beta(0)S_n/N$. A new infection will be either active or latent depending on the phenotype of the infecting strain y.

at discrete time n, and the random variable S_n is the total number of susceptible agents in the system at discrete time n computed as $S_n = N - \sum_i \sum_j [L_n(i,j) + A_n(i,j)]$, where $N \in \mathbb{N}$ is the infection carrying capacity.

In the computational algorithm, infecting strains are first allowed to mutate (or epimutate) which results in incremental changes to the strain's character. This is implemented as a random walk on the phenotype lattice such that $(i,j) \to (i+1,j), (i,j+1), (i-1,j)$ or $(i,j-1)$ during a time step with respective probability $\mu\tau/4$, so agents actually move with probability $\mu\tau$ and pause instead with probability $1-\mu\tau$. We constrain the trait variables of each agent $x \in [0,1]$ and $y \in [0,1]$ by implementing reflecting boundary conditions – if an agent at the boundary of the phenotypic domain chooses to move outside of the domain then that move is aborted and the agent retains its trait values for the duration of the time step.

Following this step, active infections regress into the latent state with probability $\omega\tau$ and latent infections reactivate with probability $a\tau$.

During the last part of each time step, infections will either

1. cause a new infection due to a transmission event with probability $\tau\beta(x)S_n/N$ for latent infections and probability $\tau\beta(0)S_n/N$ for active infections (where $\beta(x)$ and $\beta(0)$ are the respective transmission rates of a latent and active infecting strain with phenotype (x,y) in a completely susceptible host population);

2. be lost due to host recovery or host death with probability $\tau\lambda(x) = \tau\gamma(x) + \tau\theta(x)$ for latent infections and probability $\tau\lambda(0) = \tau\gamma(0) + \tau\theta(0)$ for active infections (where $\gamma(x)$ and $\theta(x)$ are the respective host-recovery and host-death rates for latent strains with phenotype (x,y) and $\gamma(0)$ and $\theta(0)$ are the respective host-recovery and host-death rates for all active strains);

3. do nothing with probability $1 - \tau[\beta(x)S_n/N - \lambda(x)]$ for latent infections and probability $1 - \tau[\beta(0)S_n/N - \lambda(0)]$ for active infections."

We make the assumption that new infections always inherit the phenotype (x,y) of the infecting strain. However, new infections will be initially active with probability $1-y$, while with probability y a new infection will be initially latent. For our simulations we chose a decreasing $\beta(x)$ since we expect that more latent infections will always be less transmissible for *M. tuberculosis*.

Of interest are the values of the population mean trait values, given respectively by

$$\langle x_n \rangle = \frac{1}{N - S_n} \sum_i \sum_j i\Delta[L_n(i,j) + A_n(i,j)],$$
$$\langle y_n \rangle = \frac{1}{N - S_n} \sum_i \sum_j j\Delta[L_n(i,j) + A_n(i,j)].$$

These determine the evolutionary trajectory of the population of infections through time.

Finally, we consider only cases where

$$a > 0, \quad \omega > 0, \quad \theta(x) > 0, \quad \gamma(x) \geq 0, \quad \beta(x) \geq 0, \quad 0 \leq y \leq 1. \tag{A.1}$$

These assumptions correspond to scenarios where there are non-zero activation, regression and host-death rates, but where the recovery rate and transmission rate can be zero. In the algorithm, τ is chosen small enough so that quantities interpreted as probabilities fall within the interval $(0,1)$.

B. Continuum model of M. tuberculosis evolution

An analysis of the continuum limit of the discrete model that we have simulated is now provided and shows how the integrodifferential equation model emerges under appropriate approximations.

We denote by $I(q,p)$ an indicator random variable associated with an event q involving a single agent, which takes the value 1 with probability p and is zero otherwise. The event q may be subscripted. In a sum over k involving q_k, the events for distinct values of k are assumed independent. Even if bearing the same value of the subscript, events appearing in summations with different dummy indices of summation are also assumed independent (an abuse of notation that avoids ugly symbolism).

We denote by $L_n^{\ddagger}(i,j)$ the number of latent agents with phenotype (i,j) when the agents have just updated their phenotype due to (epi)mutations (that occur at a rate $P=\mu\tau$ per time step) before any active/latent subpopulation switching has occurred, and before any transmission or infection-loss events have occurred. Then

$$L_n^{\ddagger}(i,j) = L_n(i,j) + \sum_{\ell=1}^{L_n(i+1,j)} I(q_\ell, P/4) + \sum_{r=1}^{L_n(i-1,j)} I(q_r, P/4) + \sum_{d=1}^{L_n(i,j+1)} I(q_d, P/4) + \sum_{u=1}^{L_n(i,j-1)} I(q_u, P/4) - \sum_{k=1}^{L_n(i,j)} I(\omega_k, P),$$

where the sum over ℓ accounts for the movement choices of latent agents at phenotype $(i+1,j)$ (who must move left to become of phenotype (i,j)), the sum over r accounts for the movement choices of agents at phenotype $(i-1,j)$ (who must move right to become of phenotype (i,j)), the sum over d accounts for the movement choices of agents at phenotype $(i,j+1)$ (who must move down to become of phenotype (i,j)), the sum over u accounts for the movement choices of agents at phenotype $(i,j-1)$ (who must move up to become of phenotype (i,j)) and the sum over k accounts for those agents currently of phenotype (i,j) that mutate. Averaging over many statistically identical realisations (denoted by angle brackets), we find that

$$\langle L_n^{\ddagger}(i,j)\rangle = \langle L_n(i,j)\rangle - P\langle L_n(i,j)\rangle + P/4\{\langle L_n(i+1,j)\rangle + \langle L_n(i-1,j)\rangle + \langle L_n(i,j+1)\rangle + \langle L_n(i,j-1)\rangle\}. \tag{B.1}$$

Analogously, if we denote by $A_n^{\ddagger}(i,j)$ the number of active agents with phenotype (i,j) when the agents have just updated their phenotype due to (epi)mutations, before any active/latent subpopulation switching has occurred, and before any transmission or infection loss events have occurred, then it can be shown that

$$\langle A_n^{\ddagger}(i,j)\rangle = \langle A_n(i,j)\rangle - P\langle A_n(i,j)\rangle + P/4\{\langle A_n(i+1,j)\rangle + \langle A_n(i-1,j)\rangle\langle A_n(i,j+1)\rangle + \langle A_n(i,j-1)\rangle\}. \tag{B.2}$$

We now consider the stochastic switching of agents between the active and latent subpopulations. Latent agents switch to active agents with probability $a\tau$ while active agents switch to latent agents with probability $\omega\tau$. If $L_n^{\ddagger}(i,j)=\phi$ and $A_n^{\ddagger}(i,j)=\xi$ then the expected number of latent agents of phenotype (i,j) that switch to the active subpopulation after the stochastic switching stage at time n is $a\tau\phi$, while the expected number of active agents of phenotype (i,j) that switch to the latent subpopulation after the stochastic switching stage at time n is $\omega\tau\xi$. Hence, if we denote by $L_n^{*}(i,j)$ the number of latent agents with phenotype (i,j) when the agents have just undergone active/latent

subpopuation switching, and before any transmission or infection-loss events have occurred, we find that

$$\langle L_n^*(i,j)\rangle = \sum_{\xi}\sum_{\phi}\big[(1-a\tau)\phi + \omega\tau\xi\big]\Pr\{L_n^\ddagger(i,j)=\phi, A_n^\ddagger(i,j)=\xi\}.$$

Analogously, if we denote by $A_n^*(i,j)$ the number of active agents with phenotype (i,j) when the agents have just undergone active/latent subpopuation switching, and before any transmission or infection-loss events have occurred, we find that

$$\langle A_n^*(i,j)\rangle = \sum_{\xi}\sum_{\phi}\big[(1-\omega\tau)\xi + a\tau\phi\big]\Pr\{L_n^\ddagger(i,j)=\phi, A_n^\ddagger(i,j)=\xi\}.$$

Hence we find that

$$\langle L_n^*(i,j)\rangle = (1-a\tau)\langle L_n^\ddagger(i,j)\rangle + \omega\tau\langle A_n^\ddagger(i,j)\rangle, \tag{B.3}$$

$$\langle A_n^*(i,j)\rangle = (1-\omega\tau)\langle A_n^\ddagger(i,j)\rangle + a\tau\langle L_n^\ddagger(i,j)\rangle. \tag{B.4}$$

We now consider the transmission and infection loss events for current agents. We denote by $\beta_n(i)$ and $\lambda_n(i)$ the respective transmission and infection loss rates for current latent agents at time step n with phenotype coordinate (i,j). Similarly, we denote by $\beta_n(0)$ and $\lambda_n(0)$ the respective transmission and infection loss rates for current active agents at time step n with phenotype coordinate (i,j). For each latent agent we assume the agent either:

(i) divides into two latent agents with phenotype (i,j) with probability

$$\tau j\Delta\beta_n(i)\mathcal{S}(\sum_i\sum_j[L_n^*(i,j)+A_n^*(i,j)]);$$

(ii) divides into one latent agent and one active agent with phenotypes (i,j) with probability

$$\tau(1-j\Delta)\beta_n(i)\mathcal{S}(\sum_i\sum_j[L_n^*(i,j)+A_n^*(i,j)]);$$

(iii) is lost with probability $\tau\lambda_n(i)$;

(iv) does nothing (and so remains in place) with probability

$$1-\tau\beta_n(i)\mathcal{S}(\sum_i\sum_j[L_n^*(i,j)+A_n^*(i,j)])-\tau\lambda_n(i).$$

For each active agent we assume the agent either:

(i) divides into two active agents with phenotype (i,j) with probability

$$\tau(1-j\Delta)\beta_n(0)\mathcal{S}(\sum_i\sum_j[L_n^*(i,j)+A_n^*(i,j)]);$$

(ii) divides into one latent agent and one active agent with phenotypes (i,j) with probability

$$\tau j\Delta\beta_n(0)\mathcal{S}(\sum_i\sum_j[L_n^*(i,j)+A_n^*(i,j)]);$$

(iii) is lost with probability $\tau\lambda_n(0)$;

(iv) does nothing (and so remains in place) with probability

$$1-\tau\beta_n(0)\mathcal{S}(\sum_i\sum_j[L_n^*(i,j)+A_n^*(i,j)])-\tau\lambda_n(0).$$

We remark that $\sum_i\sum_j[L_n^*(i,j)+A_n^*(i,j)]$ is a random variable for which the expected value is taken as $\varrho(t)$ in the continuum limit, and our primary interest is in the case $\mathcal{S}(\varrho)=1-\varrho/N$.

If $\sum_i\sum_j[L_n^*(i,j)+A_n^*(i,j)]=\eta$, $L_n^*(i,j)=\nu$ and $A_n^*(i,j)=\psi$ then the expected number of latent agents of phenotype (i,j) at time $n+1$ is

$$\langle L_{n+1}(i,j)\rangle=\sum_{\eta,\psi,\nu}\Big(\nu\big[1+j\Delta\tau\beta_n(i)\mathcal{S}(\eta)-\tau\lambda_n(i)\big]+\psi j\Delta\tau\beta_n(0)\mathcal{S}(\eta)\Big)\\ \times\Pr\{L_n^*(i,j)=\nu,A_n^*(i,j)=\psi,\sum_i\sum_j[L_n^*(i,j)+A_n^*(i,j)]=\eta\},$$

and the expected number of active agents of phenotype (i,j) at time $n+1$ is

$$\langle A_{n+1}(i,j)\rangle=\sum_{\eta,\psi,\nu}\Big(\psi\big[1+(1-j\Delta)\tau\beta_n(0)\mathcal{S}(\eta)-\tau\lambda_n(0)\big]+\nu(1-j\Delta)\tau\beta_n(i)\mathcal{S}(\eta)\Big)\\ \times\Pr\{L_n^*(i,j)=\nu,A_n^*(i,j)=\psi,\sum_i\sum_j[L_n^*(i,j)+A_n^*(i,j)]=\eta\}.$$

We now invoke a single probabilistic approximation, which is of the mean-field type frequently used for the analysis of agent-based systems: in the summands we replace

$$\mathcal{S}(\eta)=\mathcal{S}(\sum_i\sum_j[L_n^*(i,j)+A_n^*(i,j)]),$$

by

$$\mathcal{S}(\langle\sum_i\sum_j[L_n^*(i,j)+A_n^*(i,j)]\rangle),$$

and we note that as

$$\langle\sum_i\sum_j[L_n^*(i,j)+A_n^*(i,j)]\rangle=\langle\sum_i\sum_j[L_n(i,j)+A_n(i,j)]\rangle=\varrho$$

(since the transition from $L_n(i,j)$ to $L_n^*(i,j)$ and from $A_n(i,j)$ to $A_n^*(i,j)$ in the simulation does not change total agent numbers) we have

$$\langle L_{n+1}(i,j)\rangle\approx\big[1+j\Delta\tau\beta_n(i)\mathcal{S}(\varrho)-\tau\lambda_n(i)\big]\langle L_n^*(i,j)\rangle+j\Delta\tau\beta_n(0)\mathcal{S}(\varrho)\langle A_n^*(i,j)\rangle, \tag{B.5}$$

$$\langle A_{n+1}(i,j)\rangle\approx\big[1+(1-j\Delta)\tau\beta_n(0)\mathcal{S}(\varrho)-\tau\lambda_n(0)\big]\langle A_n^*(i,j)\rangle+(1-j\Delta)\tau\beta_n(i)\mathcal{S}(\varrho)\langle L_n^*(i,j)\rangle. \tag{B.6}$$

If we eliminate $\langle L_n^\ddagger(i,j)\rangle$, $\langle A_n^\ddagger(i,j)\rangle$, $\langle L_n^*(i,j)\rangle$ and $\langle A_n^*(i,j)\rangle$ from Eqs (B.1)–(B.6) and take $t=n\tau$, $x=\Delta i$, $y=\Delta j$, $\Delta^2L(x,y,t)=\langle L_n(i,j)\rangle$ and $\Delta^2A(x,y,t)=\langle A_n(i,j)\rangle$ we have

$$\begin{aligned}L(x,y,t+\tau)&=\big\{1+\tau y\beta_n(i)\mathcal{S}(\varrho)-\tau\lambda_n(i)-a\tau+a\tau\big[\tau y\beta_n(0)\mathcal{S}(\varrho)-y\tau\beta_n(i)\mathcal{S}(\varrho)+\tau\lambda_n(i)\big]\big\}\\&\quad\times\big\{(1-P)L(x,y,t)+P/4\big[L(x+\Delta,y,t)+L(x-\Delta,y,t)+L(x,y+\Delta,t)+L(x,y-\Delta,t)\big]\big\}\\&\quad+\big\{\tau y\beta_n(0)\mathcal{S}(\varrho)+\omega\tau+\omega\tau\big[\tau y\beta_n(i)\mathcal{S}(\varrho)-\tau\lambda_n(i)-y\tau\beta_n(0)\mathcal{S}(\varrho)\big]\big\}\\&\quad\times\big\{(1-P)A(x,y,t)+P/4\big[A(x+\Delta,y,t)+A(x-\Delta,y,t)+A(x,y+\Delta,t)+A(x,y-\Delta,t)\big]\big\},\end{aligned}$$

$$
\begin{aligned}
A(x,y,t+\tau) &= \big\{1+\tau(1-y)\beta_n(0)\mathcal{S}(\varrho)-\tau\lambda_n(0)-\omega\tau+\omega\tau\big[\tau(1-y)\beta_n(i)\mathcal{S}(\varrho)-(1-y)\tau\beta_n(0)\mathcal{S}(\varrho)+\tau\lambda_n(0)\big]\big\}\\
&\times\big\{(1-P)A(x,y,t)+P/4\big[A(x+\Delta,y,t)+A(x-\Delta,y,t)+A(x,y+\Delta,t)+A(x,y-\Delta,t)\big]\big\}\\
&+\big\{\tau(1-y)\beta_n(i)\mathcal{S}(\varrho)+a\tau+a\tau\big[\tau(1-y)\beta_n(0)\mathcal{S}(\varrho)-\tau\lambda_n(0)-(1-y)\tau\beta_n(i)\mathcal{S}(\varrho)\big]\big\}\\
&\times\big\{(1-P)L(x,y,t)+P/4\big[L(x+\Delta,y,t)+L(x-\Delta,y,t)+L(x,y+\Delta,t)+L(x,y-\Delta,t)\big]\big\}.
\end{aligned}
$$

Expanding L and A as Taylor series we have

$$
\begin{aligned}
L(x,y,t+\tau) &= \big\{1+\tau y\beta_n(i)\mathcal{S}(\varrho)-\tau\lambda_n(i)-a\tau+a\tau\big[\tau y\beta_n(0)\mathcal{S}(\varrho)-y\tau\beta_n(i)\mathcal{S}(\varrho)+\tau\lambda_n(i)\big]\big\}\\
&\times\big\{(L(x,y,t)+\frac{P\Delta^2}{4}\left[\frac{\partial^2 L}{\partial x^2}+\frac{\partial^2 L}{\partial y^2}\right]+o(\Delta^2)\big\}\\
&+\big\{\tau y\beta_n(0)\mathcal{S}(\varrho)+\omega\tau+\omega\tau\big[\tau y\beta_n(i)\mathcal{S}(\varrho)-\tau\lambda_n(i)-y\tau\beta_n(0)\mathcal{S}(\varrho)\big]\big\}\\
&\times\big\{A(x,y,t)+\frac{P\Delta^2}{4}\left[\frac{\partial^2 A}{\partial x^2}+\frac{\partial^2 A}{\partial y^2}\right]+o(\Delta^2)\big\},\\
A(x,y,t+\tau) &= \big\{1+\tau(1-y)\beta_n(0)\mathcal{S}(\varrho)-\tau\lambda_n(0)-\omega\tau+\omega\tau\big[\tau(1-y)\beta_n(i)\mathcal{S}(\varrho)-(1-y)\tau\beta_n(0)\mathcal{S}(\varrho)+\tau\lambda_n(0)\big]\big\}\\
&\times\big\{A(x,y,t)+\frac{P\Delta^2}{4}\left[\frac{\partial^2 A}{\partial x^2}+\frac{\partial^2 A}{\partial y^2}\right]+o(\Delta^2)\big\}\\
&+\big\{\tau(1-y)\beta_n(i)\mathcal{S}(\varrho)+a\tau+a\tau\big[\tau(1-y)\beta_n(0)\mathcal{S}(\varrho)-\tau\lambda_n(0)-(1-y)\tau\beta_n(i)\mathcal{S}(\varrho)\big]\big\}\\
&\times\big\{L(x,y,t)+\frac{P\Delta^2}{4}\left[\frac{\partial^2 L}{\partial x^2}+\frac{\partial^2 L}{\partial y^2}\right]+o(\Delta^2)\big\}.
\end{aligned}
$$

Hence, writing $\beta_n(i)=\beta(x)$ and $\lambda_n(i)=\lambda(x)$,

$$
\begin{aligned}
\frac{L(x,y,t+\tau)-L(x,y,t)}{\tau} &= \frac{P\Delta^2}{4\tau}\left[\frac{\partial^2 L}{\partial x^2}+\frac{\partial^2 L}{\partial y^2}\right]+o\Big(\frac{\Delta^2}{\tau}\Big)+[y\beta(x)\mathcal{S}(\varrho)-\lambda(x)-a+a\tau y\beta(0)\mathcal{S}(\varrho)\\
&-ay\tau\beta(x)\mathcal{S}(\varrho)+a\tau\lambda(x))]\times\Big[L(x,y,t)+\frac{P\Delta^2}{4}\left[\frac{\partial^2 L}{\partial x^2}+\frac{\partial^2 L}{\partial y^2}\right]+o(\Delta^2)\Big]\\
&+[y\beta(0)\mathcal{S}(\varrho)+\omega+\omega\tau y\beta(x)\mathcal{S}(\varrho)-\omega y\tau\beta(0)\mathcal{S}(\varrho)-\omega\tau\lambda(x)]\\
&\times\Big[A(x,y,t)+\frac{P\Delta^2}{4}\left[\frac{\partial^2 A}{\partial x^2}+\frac{\partial^2 A}{\partial y^2}\right]+o(\Delta^2)\Big],\\
\frac{A(x,y,t+\tau)-A(x,y,t)}{\tau} &= \frac{P\Delta^2}{4\tau}\left[\frac{\partial^2 A}{\partial x^2}+\frac{\partial^2 A}{\partial y^2}\right]+o\Big(\frac{\Delta^2}{\tau}\Big)+[(1-y)\beta(0)\mathcal{S}(\varrho)-\lambda(0)-\omega+\omega\tau(1-y)\beta(x)\mathcal{S}(\varrho)\\
&-\omega(1-y)\tau\beta(0)\mathcal{S}(\varrho)+\omega\tau\lambda(0)]\times\Big[A(x,y,t)+\frac{P\Delta^2}{4}\left[\frac{\partial^2 A}{\partial x^2}+\frac{\partial^2 A}{\partial y^2}\right]+o(\Delta^2)\Big]\\
&+[(1-y)\beta(x)\mathcal{S}(\varrho)+a+a\tau(1-y)\beta(0)\mathcal{S}(\varrho)-a(1-y)\tau\beta(x)\mathcal{S}(\varrho)-a\tau\lambda(0)]\\
&\times\Big[L(x,y,t)+\frac{P\Delta^2}{4}\left[\frac{\partial^2 L}{\partial x^2}+\frac{\partial^2 L}{\partial y^2}\right]+o(\Delta^2)\Big].
\end{aligned}
$$

To facilitate the emergence of a sensible continuum limit we assume that

$$
\lim_{\Delta,\tau\to 0}\frac{P\Delta^2}{4\tau}=D,
$$

and so

$$
\begin{aligned}
\frac{\partial L}{\partial t} &= D\nabla^2 L+\Big[-a+\lim_{\Delta,\tau\to 0}\Big(y\beta(x)\mathcal{S}(\varrho)-\lambda(x)\Big)\Big]L+\Big[\omega+\lim_{\Delta,\tau\to 0}\Big(y\beta(0)\mathcal{S}(\varrho)\Big)\Big]A,\\
\frac{\partial A}{\partial t} &= D\nabla^2 A+\Big[-\omega+\lim_{\Delta,\tau\to 0}\Big((1-y)\beta(0)\mathcal{S}(\varrho)-\lambda(0)\Big)\Big]A+\Big[a+\lim_{\Delta,\tau\to 0}\Big((1-y)\beta(x)\mathcal{S}(\varrho)\Big)\Big]L,
\end{aligned}
$$

where

$$\varrho(t) = \int_{-\infty}^{\infty}\int_{-\infty}^{\infty}[L(x,y,t) + A(x,y,t)]dxdy. \tag{B.7}$$

For our simulations

$$\mathcal{S}(\varrho) = 1 - \varrho/N$$

and we arrive at the system of integrodifferential equations

$$\begin{aligned}
\frac{\partial L}{\partial t} &= L(x,y,t)\Big(\underbrace{y\beta(x)\mathcal{S}(\varrho)}_{\substack{\text{transmission from}\\ \text{latent infection}}} - \underbrace{\gamma(x)}_{\text{recovery}} - \underbrace{\theta(x)}_{\substack{\text{host}\\ \text{death}}} - \underbrace{a}_{\text{reactivation}} \Big) \\
&\quad + A(x,y,t)\Big(\underbrace{y\beta(0)\mathcal{S}(\varrho)}_{\substack{\text{transmission from}\\ \text{active infection}}} + \underbrace{\omega}_{\text{regression}} \Big) + \underbrace{D\nabla^2 L(x,y,t),}_{\substack{\text{stochastic variation}\\ \text{in phenotype}}} \\
\frac{\partial A}{\partial t} &= A(x,y,t)\Big(\underbrace{(1-y)\beta(0)\mathcal{S}(\varrho)}_{\substack{\text{transmission from}\\ \text{active infection}}} - \underbrace{\gamma(0)}_{\text{recovery}} - \underbrace{\theta(0)}_{\substack{\text{host}\\ \text{death}}} - \underbrace{\omega}_{\text{regression}} \Big) \\
&\quad + L(x,y,t)\Big(\underbrace{(1-y)\beta(x)\mathcal{S}(\varrho)}_{\substack{\text{transmission from}\\ \text{latent infection}}} + \underbrace{a}_{\text{reactivation}} \Big) + \underbrace{D\nabla^2 A(x,y,t).}_{\substack{\text{stochastic variation}\\ \text{in phenotype}}}
\end{aligned} \tag{B.8}$$

The preceding analysis should be performed on the finite domain $(x, y) \in [0, 1]^2$, with τ chosen small enough so that quantities interpreted as probabilities fall in the interval $(0, 1)$. We have found that a close quantitative correspondence between simulations of the agent-based model on the finite phenotypic domain $(x, y) \in [0, 1]^2$ and numerical solutions of the integrodifferential equation model (B.7)–(B.8) can be found by imposing zero-Neumann boundary conditions (compare Panels A, C and E in Figure 2 with those in Figure S2) and choosing a lattice spacing $\Delta = 0.01$ and time step $\tau = 0.01$. Although the link between the agent-based and continuum models requires $\Delta \to 0^+$ and $\tau \to 0^+$.

Of interest are the values of the average population mean trait values, given respectively by

$$\begin{aligned}
\langle x(t)\rangle &= \frac{1}{\varrho(t)}\int_0^1\int_0^1 x[L(x,y,t) + A(x,y,t)]\mathrm{d}x\mathrm{d}y, \\
\langle y(t)\rangle &= \frac{1}{\varrho(t)}\int_0^1\int_0^1 y[L(x,y,t) + A(x,y,t)]\mathrm{d}x\mathrm{d}y.
\end{aligned}$$

It can be shown that $A(\cdot,\cdot,t) + L(\cdot,\cdot,t)$ remains bounded in our model. We assume $A(x, y, t = 0)$ and $L(x, y, t = 0)$ are non-negative functions with compact support in $L^1 \cap L^\infty(\Omega)$, zero-Neumann boundary conditions, the parameter functions $\beta(\cdot)$, $\gamma(\cdot)$ and $\theta(\cdot)$ are sufficiently smooth, and there exists some non-negative real constants $\overline{\beta}$, $\underline{\beta}$, $\overline{\gamma}$, $\underline{\gamma}$, $\overline{\theta}$ and $\underline{\theta}$ such that

$$0 \le \underline{\beta} \le \beta(\cdot) \le \overline{\beta} < \infty, \qquad 0 \le \underline{\gamma} \le \gamma(\cdot) \le \overline{\gamma} < \infty, \qquad 0 < \underline{\theta} \le \theta(\cdot) \le \overline{\theta} < \infty.$$

In our model, A and L are non-negative. If we sum the two PDE equations in the model (B.8) together to obtain

$$\frac{\partial(L + A)}{\partial t} = L[\beta(x)\mathcal{S}(\varrho) - \gamma(x) - \theta(x)] + A[\beta(0)\mathcal{S}(\varrho) - \gamma(0) - \theta(0)] + D\nabla^2(L + A),$$

and substitute the definition

$$\mathcal{S}(\varrho) := 1 - \frac{\varrho(t)}{N} \quad \text{with} \quad \varrho(t) = \int\int_\Omega \big[L(x,y,t) + A(x,y,t)\big]dxdy,$$

into the above equation we achieve

$$\frac{d\varrho}{dt} = \int\int_\Omega \left\{ L\left[\beta(x)\left(1-\frac{\varrho}{N}\right) - \gamma(x) - \theta(x)\right] + A\left[\beta(0)\left(1-\frac{\varrho}{N}\right) - \gamma(0) - \theta(0)\right]\right\} dxdy,$$

Because of the non-negativity of A and L, we have

$$\frac{d\varrho}{dt} \le \int\int_\Omega \left[L\beta(x)\left(1-\frac{\varrho}{N}\right) + A\beta(0)\left(1-\frac{\varrho}{N}\right)\right] dxdy - \big(\underline{\gamma} + \underline{\theta}\big)\varrho.$$

Hence, if $\varrho(t) = N$,

$$\frac{d\varrho(t)}{dt} \le -(\underline{\theta} + \underline{\gamma})\ \varrho(t) < 0.$$

The above differential inequality allows us to conclude that $\varrho(t) \le N$ for all $t > 0$ and $A(\cdot,\cdot,t) + L(\cdot,\cdot,t)$ is bounded in $L^1(\Omega)$ for all $t \ge 0$.

C. Derivation of the basic reproductive number R_0

The next generation method [1] is used to derive the basic reproductive number R_0 when the phenotype-space length scale of the discrete stochastic model approaches zero $\Delta \to 0^+$. This technique is suitable for models where there are more than one class of infectives.

Following the method outlined in [1], we define $F_L(L(x,y), A(x,y))$ to be the rate of appearance of new individual infections in the latent population with phenotype (x,y), and $F_A(L(x,y), A(x,y))$ to be the rate of appearance of new individual infections in the active population with phenotype (x,y) so that

$$\begin{aligned} F_L(L(x,y), A(x,y)) &= y\beta(x)L(x,y) + y\beta(0)A(x,y) \\ F_A(L(x,y), A(x,y)) &= (1-y)\beta(x)L(x,y) + (1-y)\beta(0)A(x,y). \end{aligned}$$

We also define

$$V_L(L(x,y), A(x,y)) := V_L^-(L(x,y), A(x,y)) - V_L^+(L(x,y), A(x,y)),$$

where $V_L^+(L(x,y), A(x,y))$ is the rate of transfer of individual infections into the latent population with phenotype (x,y) by all other means and $V_L^-(L(x,y), A(x,y))$ is the rate of transfer of individual infections out of the latent population with phenotype (x,y). Similarly, we define

$$V_A(L(x,y), A(x,y)) := V_A^-(L(x,y), A(x,y)) - V_A^+(L(x,y), A(x,y)),$$

where $V_A^+(L(x,y), A(x,y))$ is the rate of transfer of individual infections into the active population by all other means and $V_A^-(L(x,y), A(x,y))$ is the rate of transfer of individual infections out of the active population so that

$$\begin{aligned} V_L(L(x,y), A(x,y)) &= L(x,y)[\lambda(x) + a + \mu] - \omega A(x,y) \\ &\quad - \frac{\mu}{4}[L(x+\Delta,y) + L(x-\Delta,y) + L(x,y+\Delta) + L(x,y-\Delta)], \\ V_A(L(x,y), A(x,y)) &= A(x,y)[\lambda(0) + \omega + \mu] - aL(x,y) \\ &\quad - \frac{\mu}{4}[A(x+\Delta,y) + A(x-\Delta,y) + A(x,y+\Delta) + A(x,y-\Delta)]. \end{aligned}$$

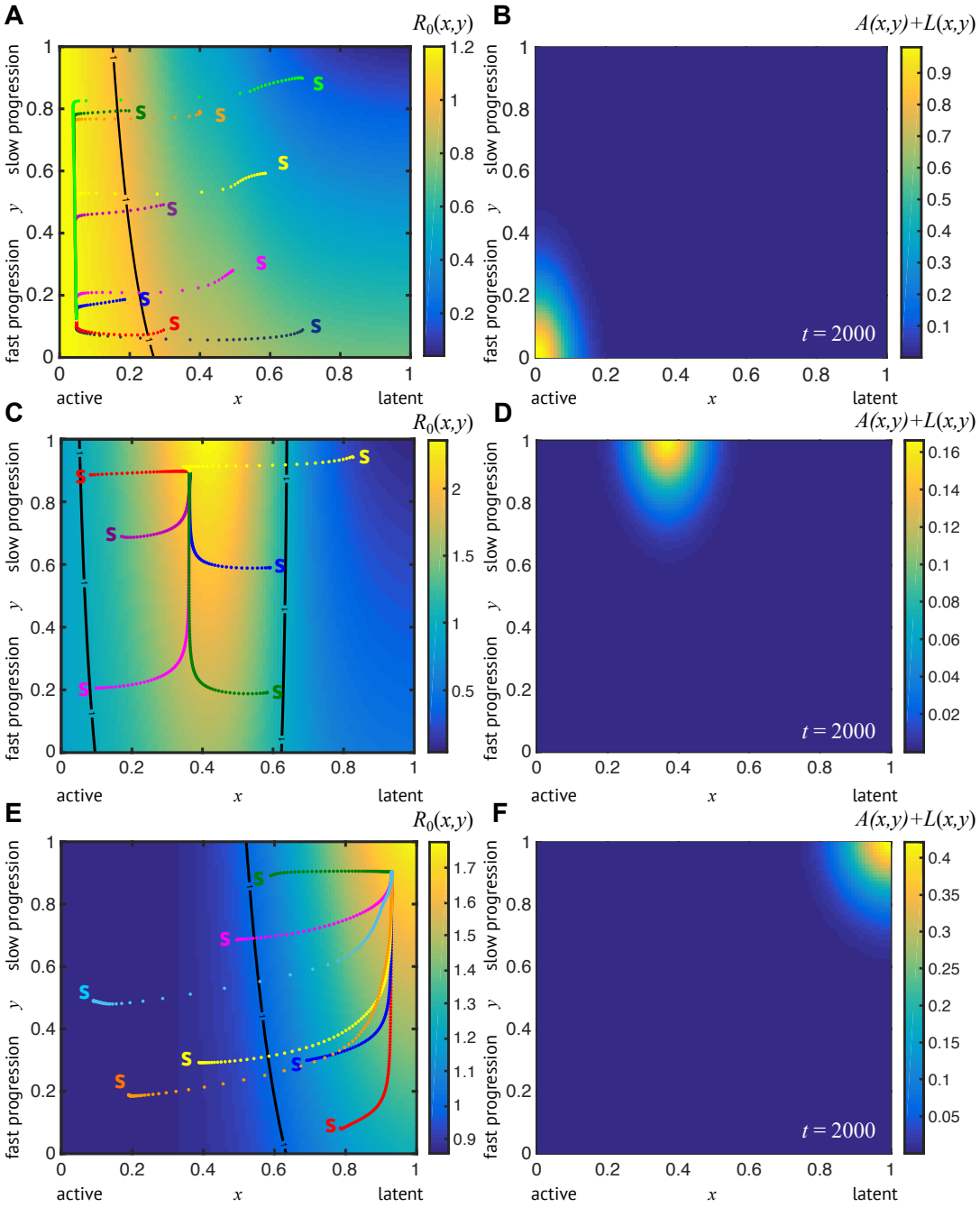

Figure S2: The basic reproductive number R_0 of a pathogen acts as a heuristic for predicting evolutionary trajectories. When R_0 has the form shown in Eq. (1) either active disease is favoured (A); an intermediate level of latency is favoured with slow progression (C); or latency is favoured with slow progression, (E). Panels B, D, and F display a density plot of the equilibrium phenotype distribution (*i.e.*, $L(x, y, 2000) + A(x, y, 2000)$) for the cases corresponding to the respective fitness landscapes shown in Panels A, C and E. Panels A, C and E also display the trajectories of the average population mean trait values computed from numerical solutions of the integrodifferential equation model (Eq. (2)) as coloured dotted lines superimposed over the associated density plot of R_0. The initial population mean trait values of the populations are indicated by their respective coloured "s". The integrodifferential equation model cannot capture extinction. Therefore all of the average population mean trait values of the pathogen populations stabilise in the region of the global maximum of R_0. The black lines indicate the contour $R_0 = 1$. The forms of parameters as functions of potential latency x and other parameter values are provided in Section G.

Here, $\lambda(\cdot) = \gamma(\cdot) + \theta(\cdot)$. Expanding L and A as Taylor series we have

$$\begin{aligned}
V_L(L(x,y),A(x,y)) &= L(x,y)[\lambda(x) + a + \mu] - \omega A(x,y) \\
&\quad - \frac{\mu}{4}[4L(x,y) + \Delta^2 \frac{\partial^2 L}{\partial x^2}(x,y) + \Delta^2 \frac{\partial^2 L}{\partial y^2}(x,y) + o(\Delta^2)], \\
V_A(L(x,y),A(x,y)) &= A(x,y)[\lambda(0) + \omega + \mu] - aL(x,y) \\
&\quad - \frac{\mu}{4}[4A(x,y) + \Delta^2 \frac{\partial^2 A}{\partial x^2}(x,y) + \Delta^2 \frac{\partial^2 A}{\partial y^2}(x,y) + o(\Delta^2)].
\end{aligned}$$

When we take the limit $\Delta \to 0^+$ we see that

$$\begin{aligned}
V_L(L(x,y),A(x,y)) &= L(x,y)[\lambda(x) + a] - \omega A(x,y), \\
V_A(L(x,y),A(x,y)) &= A(x,y)[\lambda(0) + \omega] - aL(x,y).
\end{aligned}$$

We form the next generation matrix operator FV^{-1} from the matrices of partial derivatives of F_L, F_A, V_L and V_A:

$$\begin{aligned}
F &= \begin{bmatrix} \partial_L F_L & \partial_A F_L \\ \partial_L F_A & \partial_A F_A \end{bmatrix} = \begin{bmatrix} y\beta(x) & y\beta(0) \\ (1-y)\beta(x) & (1-y)\beta(0) \end{bmatrix}, \\
V &= \begin{bmatrix} \partial_L V_L & \partial_A V_L \\ \partial_L V_A & \partial_A V_A \end{bmatrix} = \begin{bmatrix} \lambda(x) + a & -\omega \\ -a & \lambda(0) + \omega \end{bmatrix}.
\end{aligned}$$

and then calculate R_0 as the largest eigenvalue of the matrix FV^{-1}. We find that

$$R_0(x,y) = \frac{\{\beta(x)[\lambda(0)y + \omega] + \beta(0)[a + (1-y)\lambda(x)]\}}{a\lambda(0) + \lambda(x)[\omega + \lambda(0)]}. \tag{C.1}$$

To interpret the meaning of R_0, we rewrite Equation (C.1) in the following form:

$$\begin{aligned}
R_0(x,y) = {} & \underbrace{(1-y)}_{\substack{\text{probability a new} \\ \text{infection is active}}} \left\{ \underbrace{\frac{\beta(0)}{\lambda(0) + \omega\left(\frac{\lambda(x)}{\lambda(x)+a}\right)}}_{\substack{\text{expected number of secondary} \\ \text{cases due to an active infection}}} + \underbrace{\left(\frac{\omega}{\lambda(0)+\omega}\right)}_{\substack{\text{probability of} \\ \text{regression}}} \times \underbrace{\frac{\beta(x)}{\lambda(x) + a\left(\frac{\lambda(0)}{\lambda(0)+\omega}\right)}}_{\substack{\text{expected number of secondary} \\ \text{cases due to a latent infection}}} \right\}, \\
& + \underbrace{y}_{\substack{\text{probability a new} \\ \text{infection is latent}}} \left\{ \underbrace{\frac{\beta(x)}{\lambda(x) + a\left(\frac{\lambda(0)}{\lambda(0)+\omega}\right)}}_{\substack{\text{expected number of secondary} \\ \text{cases due to a latent infection}}} + \underbrace{\left(\frac{a}{\lambda(x)+a}\right)}_{\substack{\text{probability of} \\ \text{activation}}} \times \underbrace{\frac{\beta(0)}{\lambda(0) + \omega\left(\frac{\lambda(x)}{\lambda(x)+a}\right)}}_{\substack{\text{expected number of secondary} \\ \text{cases due to an active infection}}} \right\},
\end{aligned} \tag{C.2}$$

where, the terms

$$\frac{\lambda(x)}{\lambda(x)+a}, \qquad \frac{\lambda(0)}{\lambda(0)+\omega},$$

can be interpreted as the respective probabilities that latent infections do not reactivate, and active infections do not regress to latency. Contributions to the basic reproductive number can be separated into those coming from active infections [top line of Equation (C.2)] and those coming from latent infections [bottom line of Equation (C.2)]. We see that the active infection contribution is proportional to the probability a new infections is active and a quantity that is made up the expected number of secondary cases due to an active infection, plus the probability of regression multiplied by the expected number of secondary cases due to a latent infection. Similarly, the latent infection contribution is proportional to the probability a new infections is latent and a quantity that is made up the expected number of secondary cases due to a latent infection, plus the probability of activation multiplied by the expected number of secondary cases due to an active infection.

D. Invasion analysis

To study the long-term dynamics of our model, we perform an invasion analysis. We are interested in determining the fate of a resident strain once a mutant strain appears in the population of infections.

We consider a resident strain and mutant strain with respective phenotypes (x_1, y_1) and (x_2, y_2). A_1 and L_1 represent the respective number of active and latent infections of the resident strain, while A_2 and L_2 denote the respective number of active and latent infections of the mutant strain.

In this setting, resident strains have a transmission rate $\beta_1 = \beta(x_1)$, recovery rate $\gamma_1 = \gamma(x_1)$ and host-death rate $\theta_1 = \theta(x_1)$. Similarly, mutant strains have a transmission rate $\beta_2 = \beta(x_2)$, recovery rate $\gamma_2 = \gamma(x_2)$ and host-death rate $\theta_2 = \theta(x_2)$. For convenience we define $\beta_0 = \beta(0)$, $\theta_0 = \theta(0)$, $\gamma_0 = \gamma(0)$, $\lambda_0 = \theta_0 + \gamma_0$, $\lambda_1 = \theta_1 + \gamma_1$, $\lambda_2 = \theta_2 + \gamma_2$, $R_0^{(1)} = R_0(x_1, y_1)$ and $R_0^{(2)} = R_0(x_2, y_2)$ (where R_0 is defined as in Equation (C.1)).

The dynamics are governed by the following system of equations:

$$\begin{aligned}
\frac{dA_1}{dt} &= A_1\Big\{(1-y_1)\beta_0\left[1-(A_1+A_2+L_1+L_2)/N\right]-\lambda_0-\omega\Big\} \\
&\quad + L_1\Big\{(1-y_1)\beta_1\left[1-(A_1+A_2+L_1+L_2)/N\right]+a\Big\}, && \text{(D.1)}\\
\frac{dL_1}{dt} &= L_1\Big\{y_1\beta_1\left[1-(A_1+A_2+L_1+L_2)/N\right]-\lambda_1-a\Big\} \\
&\quad + A_1\Big\{y_1\beta_0\left[1-(A_1+A_2+L_1+L_2)/N\right]+\omega\Big\}, && \text{(D.2)}\\
\frac{dA_2}{dt} &= A_2\Big\{(1-y_2)\beta_0\left[1-(A_1+A_2+L_1+L_2)/N\right]-\lambda_0-\omega\Big\} \\
&\quad + L_2\Big\{(1-y_2)\beta_2\left[1-(A_1+A_2+L_1+L_2)/N\right]+a\Big\}, && \text{(D.3)}\\
\frac{dL_2}{dt} &= L_2\Big\{y_2\beta_2\left[1-(A_1+A_2+L_1+L_2)/N\right]-\lambda_2-a\Big\} \\
&\quad + A_2\Big\{y_2\beta_0\left[1-(A_1+A_2+L_1+L_2)/N\right]+\omega\Big\}. && \text{(D.4)}
\end{aligned}$$

Consistent with the stochastic computational model outlined in Section A [conditions (A.1)], we consider only the cases where

$$N>0,\quad a>0,\quad \omega>0,\quad \lambda_i>0 \text{ for } i=0,1,2,\quad \beta_0>0,\quad \beta_i\geq 0 \text{ for } i=1,2,\quad 0\leq y_i\leq 1 \text{ for } i=1,2. \tag{D.5}$$

We determine the conditions which allow the resident strain to survive and drive the mutant strain to extinction by considering the stability of the critical point

$$(A_1, L_1, A_2, L_2) = (A, L, 0, 0), \quad \text{with} \quad A>0 \quad \text{and} \quad L>0. \tag{D.6}$$

First of all we obtain expressions for A and L based on the parameters of the problem, by substituting Equation (D.6) into Equations (D.1)–(D.4) with $\frac{dA_1}{dt}=0$, $\frac{dL_1}{dt}=0$, $\frac{dA_2}{dt}=0$ and $\frac{dL_2}{dt}=0$ to obtain

$$0 = A\Big\{(1-y_1)\beta_0\left[1-(A+L)/N\right]-\lambda_0-\omega\Big\} + L\Big\{(1-y_1)\beta_1\left[1-(A+L)/N\right]+a\Big\}, \tag{D.7}$$

$$0 = A\Big\{y_1\beta_0\left[1-(A+L)/N\right]+\omega\Big\} + L\Big\{y_1\beta_1\left[1-(A+L)/N\right]-\lambda_1-a\Big\}. \tag{D.8}$$

Adding together Equations (D.7) and (D.8), we see that

$$1-\frac{A+L}{N} = \frac{\lambda_0 A+\lambda_1 L}{A\beta_0+L\beta_1}. \tag{D.9}$$

Combining Equations (D.7) and (D.9) we obtain

$$A = L\left(\frac{a+\lambda_1(1-y_1)}{\lambda_0 y_1+\omega}\right). \tag{D.10}$$

Combining Equations (D.10) and (D.9) we arrive at

$$1-\frac{A+L}{N} = \frac{\lambda_0(a+\lambda_1)+\lambda_1\omega}{\beta_0[a+\lambda_1(1-y_1)]+\beta_1(\lambda_0 y_1+\omega)} = \frac{1}{R_0^{(1)}}. \tag{D.11}$$

Since we are interested in the case where $A>0$ and $L>0$, Equation (D.11) implies that

$$1 > 1-\frac{A+L}{N} = \frac{1}{R_0^{(1)}} \quad \Rightarrow \quad R_0^{(1)} > 1.$$

After some algebra the following expressions determine the critical point

$$\begin{aligned} A &= N\left(1-\frac{1}{R_0^{(1)}}\right)\left(\frac{a+\lambda_1(1-y_1)}{\lambda_0 y_1+\omega+a+(1-y_1)\lambda_1}\right), \\ L &= N\left(1-\frac{1}{R_0^{(1)}}\right)\left(\frac{\omega+\lambda_0 y_1}{\lambda_0 y_1+\omega+a+(1-y_1)\lambda_1}\right). \end{aligned} \tag{D.12}$$

We see that when the conditions (D.5) hold, this critical point is non-trivial only when $R_0^{(1)}>1$.

Next we determine the Jacobian matrix J for our system at the critical point given by Eq. (D.6):

$$J = \begin{pmatrix} (1-y_1)(\beta_0/R_0^{(1)}-Z)-\lambda_0-\omega & a+(1-y_1)(\beta_1/R_0^{(1)}-Z) & -(1-y_1)Z & -(1-y_1)Z \\ y_1(\beta_0/R_0^{(1)}-Z)+\omega & -a+y_1(\beta_1/R_0^{(1)}-Z)-\lambda_1 & -y_1 Z & -y_1 Z \\ 0 & 0 & (1-y_2)\beta_0/R_0^{(1)}-\lambda_0-\omega & (1-y_2)\beta_2/R_0^{(1)}+a \\ 0 & 0 & y_2\beta_0/R_0^{(1)}+\omega & y_2\beta_2/R_0^{(1)}-a-\lambda_2 \end{pmatrix}, \tag{D.13}$$

where

$$Z = \frac{A\beta_0+L\beta_1}{N} = \frac{(R_0^{(1)}-1)[\lambda_0(a+\lambda_1)+\lambda_1\omega]}{\lambda_0 y_1+\omega+a+(1-y_1)\lambda_1}.$$

Notice that $Z>0$ when $R_0^{(1)}>1$. The eigenvalues of this matrix E_1, E_2, E_3, E_4 can inform us about the stability of the critical point. In this case they take the form

$$E_1 = \frac{1}{2}\left(-c_1+\sqrt{c_1^2-4c_2}\right), \qquad E_2 = \frac{1}{2}\left(-c_1-\sqrt{c_1^2-4c_2}\right), \tag{D.14}$$

and

$$E_3 = \frac{1}{2}\left(-c_3+\sqrt{c_3^2-4c_4}\right), \qquad E_4 = \frac{1}{2}\left(-c_3-\sqrt{c_3^2-4c_4}\right), \tag{D.15}$$

where

$$\begin{aligned} c_1 &= Z+a+\lambda_0+\lambda_1+\omega-\frac{1}{R_0^{(1)}}[\beta_0(1-y_1)+\beta_1 y_1] \\ c_2 &= Z[a+y_1\lambda_0\lambda_1(1-y_1)+\omega]-\frac{1}{R_0^{(1)}}[a\beta_0+y_1\beta_1\lambda_0+(1-y_1)\beta_0\lambda_1+\beta_1\omega]+\lambda_1(\lambda_0+\omega)+a\lambda_0, \\ c_3 &= a+\lambda_0+\lambda_2+\omega-\frac{1}{R_0^{(1)}}[\beta_0(1-y_2)+\beta_2 y_2], \\ c_4 &= -\frac{1}{R_0^{(1)}}[a\beta_0+y_2\beta_2\lambda_0+(1-y_2)\beta_0\lambda_2+\beta_2\omega]+\lambda_2(\lambda_0+\omega)+a\lambda_0. \end{aligned}$$

If the the real part of each eigenvalue is negative, then the critical point is linearly stable. If $c_2 < 0$, $\Re[E_1] > 0$ and if $c_4 < 0$, $\Re[E_3] > 0$. Therefore, a necessary condition for stability is that $c_2 > 0$ and $c_4 > 0$. After some algebra, it can be shown that

- $c_2 > 0$ always hold true when our model conditions (D.5) hold and when $R_0^{(1)} > 1$, which it must for the critical point to remain nontrivial;
- $c_4 > 0$ when $R_0^{(1)} > R_0^{(2)}$.

Furthermore, it can also be shown that

- $c_1 > 0$ always holds true when our model conditions (D.5) hold;
- if $R_0^{(1)} > R_0^{(2)}$, $c_3 > 0$ when our model conditions (D.5) hold.

When $c_1 > 0$, $c_2 > 0$, $c_3 > 0$ and $c_4 > 0$, the real part of each eigenvalue E_1, E_2, E_3, E_4 is negative.

Therefore, the critical point given by Eq. (D.6) is nontrivial when $R_0^{(1)} > 1$, and stable when $R_0^{(1)} > R_0^{(2)}$. As we expected, the resident strain survives and drives the mutant strain to extinction when its basic reproductive number is greater than that of the mutant strain.

E. Analysis of the basic reproduction number R_0

In the analysis that follows, we assume the model conditions (A.1) hold true.

Internal stationary points of R_0 [given by Eq. (C.1)] occur when $\nabla R_0 = \mathbf{0}$, *i.e.*, when

$$\beta'(x)\lambda(x) - \lambda'(x)\beta(x) = \tfrac{a[\beta(0)\lambda'(x) - \beta'(x)\lambda(0)]}{\omega + \lambda(0)}, \tag{E.1}$$

$$\beta(x)\lambda(0) = \beta(0)\lambda(x). \tag{E.2}$$

Here, $\lambda(\cdot) = \gamma(\cdot) + \theta(\cdot)$. These conditions require $\beta(\cdot)$ and $\lambda(\cdot)$ to be C^1 in the domain $x \in [0, 1]$ and correspond respectively to the cases $\partial_x R_0 = 0$ and $\partial_y R_0 = 0$. Since there is no y dependence in either condition, if an internal stationary point exists it will be a line $x = x^*$ where $0 < x^* < 1$. If, on the other hand, no internal stationary points exist, then the Global Maximum of R_0 (GMR) will occur along the boundary of the phenotypic domain. Hence, to determine the GMR, we only need to consider R_0 along the edges $y = 0$ and $y = 1$. We note that Eq. (E.2) is always satisfied at $x = 0$. Therefore, R_0 is always constant along the line $x = 0$.

If a stationary point exists at $(x, y) = (x^*, y^*)$, it will be a local maximum if $\partial_{xx} R_0(x^*, y^*) < 0$, which occurs when

$$\beta''(x^*) < \beta'(x^*)\lambda''(x^*)/\lambda'(x^*). \tag{E.3}$$

If Conditions (E.1)–(E.3) hold for an x^* such that $0 < x^* < 1$ (which requires $\beta(\cdot)$ and $\lambda(\cdot)$ to be twice differentiable at $x = x^*$), then the GMR will occur along the line $x = x^*$. However, when Eq. (E.2) holds, $R_0(0, 0) = R_0(x^*, 0)$. Hence, for this case, a GMR can only occur along the line $x = x^*$ if $x = 0$ is also a GMR.

If any of the Conditions (E.1)–(E.3) are not satisfied, then the GMR will occur somewhere along the edges $y = 0$ or $y = 1$, and to determine its position will require comparing the values of $R_0(0, 0)$, $R_0(0, 1)$, $R_0(1, 0)$, $R_0(1, 1)$, $R_0(x^*, 0)$ and $R_0(x^*, 1)$, where x^* gives the position of any local maxima along either edge that satisfy Eq. (E.1) for $0 < x^* < 1$, as well as Condition (E.3).

Evaluating R_0 at the corner positions of the phenotypic domain reveals that:

$$\hat{R}_0(1,1) > \hat{R}_0(1,0) > \hat{R}_0(0,1) = \hat{R}_0(0,0), \text{ if } \tfrac{\beta(1)}{\lambda(1)} > \tfrac{\beta(0)}{\lambda(0)}, \tag{E.4}$$

$$\hat{R}_0(1,1) = \hat{R}_0(1,0) = \hat{R}_0(0,1) = \hat{R}_0(0,0), \text{ if } \tfrac{\beta(1)}{\lambda(1)} = \tfrac{\beta(0)}{\lambda(0)}, \tag{E.5}$$

$$\hat{R}_0(0,1) = \hat{R}_0(0,0) > \hat{R}_0(1,0) > \hat{R}_0(1,1), \text{ if } \tfrac{\beta(1)}{\lambda(1)} < \tfrac{\beta(0)}{\lambda(0)}. \tag{E.6}$$

Therefore, for the case when $\nexists\ x^* : 0 < x^* < 1$ that satisfies Conditions (E.1) and (E.3), we see that if

1. (E.4) holds true, the GMR occurs at $(x, y) = (1, 1)$;
2. (E.5) holds true, the GMR occur at $x = 1$ and $x = 0$;
3. (E.6) holds true, the GMR occurs at $x = 0$;

When $\exists\ x^* : 0 < x^* < 1$ that satisfies Conditions (E.1) and (E.3), local stationary points occurs at x^* along the edges $y = 0$ and $y = 1$. In this case we see that

$$\hat{R}_0(x^*,1) > \hat{R}_0(x^*,0), \text{ if } \tfrac{\beta(x^*)}{\lambda(x^*)} > \tfrac{\beta(0)}{\lambda(0)}, \tag{E.7}$$

$$\hat{R}_0(x^*,1) = \hat{R}_0(x^*,0), \text{ if } \tfrac{\beta(x^*)}{\lambda(x^*)} = \tfrac{\beta(0)}{\lambda(0)}, \tag{E.8}$$

$$\hat{R}_0(x^*,1) < \hat{R}_0(x^*,0), \text{ if } \tfrac{\beta(x^*)}{\lambda(x^*)} < \tfrac{\beta(0)}{\lambda(0)}. \tag{E.9}$$

There are nine possible ways to combine Conditions (E.4)–(E.9) when $\exists\ x^* : 0 < x^* < 1$ that satisfies Conditions (E.1) and (E.3). In this case, we see that if

1. (E.4) and (E.9) also hold true, the GMR occurs at $(x, y) = (1, 1)$ (as $R_0(0, 0) > R_0(x^*, 0)$ when (E.9) holds);
2. (E.6) and (E.7) also hold true, the GMR occurs at $(x, y) = (x^*, 1)$ (as $R_0(x^*, 1) > R_0(0, 1)$ when (E.7) holds);
3. (E.6) and (E.9) also hold true, the GMR occurs at $x = 0$ (as $R_0(0, 0) > R_0(x^*, 0)$ when (E.9) holds);
4. (E.4) and (E.7) also hold true, and

$$\begin{cases} \left(\frac{a}{\lambda(0)+\omega}\right)\{\lambda(0)[\beta(1)-\beta(x^*)]+\beta(0)[\lambda(x^*)-\lambda(1)]\} < \beta(x^*)\lambda(1)-\lambda(x^*)\beta(1), \ (x,y)=(x^*,1) \text{ is the GMR;} \\ \left(\frac{a}{\lambda(0)+\omega}\right)\{\lambda(0)[\beta(1)-\beta(x^*)]+\beta(0)[\lambda(x^*)-\lambda(1)]\} = \beta(x^*)\lambda(1)-\lambda(x^*)\beta(1), \ (x,y)=(1,1),(x^*,1) \text{ are GMR;} \\ \left(\frac{a}{\lambda(0)+\omega}\right)\{\lambda(0)[\beta(1)-\beta(x^*)]+\beta(0)[\lambda(x^*)-\lambda(1)]\} > \beta(x^*)\lambda(1)-\lambda(x^*)\beta(1), \ (x,y)=(1,1) \text{ is the GMR;} \end{cases}$$

5. (E.4) and (E.8) also hold true, the GMR occurs at $(x, y) = (1, 1)$ (as $R_0(0, 0) = R_0(x^*, 0)$ when (E.8) holds);
6. (E.6) and (E.8) also hold true, the GMR occur at $x = 0$ and $x = x^*$ (as $R_0(0, 0) = R_0(x^*, 0)$ when (E.8) holds);
7. (E.5) and (E.7) also hold true, the GMR occurs at $(x, y) = (x^*, 1)$ (as $R_0(x^*, 1) > R_0(0, 1)$ when (E.7) holds);

8. (E.5) and (E.9) also hold true, the GMR occur at $x = 0$ and $x = 1$ (as $R_0(0,0) > R_0(x^*,0)$ when (E.9) holds);

9. (E.5) and (E.8) also hold true, the GMR occur at $x = 0$, $x = x^*$ and $x = 1$ (as $R_0(0,0) = R_0(x^*,0)$ when (E.8) holds);

From the above analysis we can conclude that there are three main types of possible GMR and that these can occur at $(x,y) = (1,1)$, $(x,y) = (x^*,1)$ or $x = 0$. If a GMR exists at $x = 0$ then it is also possible to have additional global maxima at $x = x^*$ and/or $x = 1$. It is also possible to have multiple concurrent GMR at $(x,y) = (1,1)$ and $(x,y) = (x^*,1)$.

If we view R_0 as an *M. tuberculosis* fitness landscape, then these results correspond to the following evolutionary scenarios. Either:

- latency is favoured with slow progression;
- an intermediate degree of latency is favoured with slow progression;
- active disease is favoured and the speed of progression is not under selection;
- active disease and either full or intermediate degrees of latency are equally favoured with no selective pressure on the speed of progression;
- active disease, intermediate degrees of latency and full latency are equally favoured with no selective pressure on the speed of progression;
- intermediate degrees of latency and full latency are equally favoured with slow progression.

Therefore, slow progression ($y = 1$) is favoured when some degree of latency is the optimal persistence strategy. Intuitively this makes sense as it is not logical for a pathogen to cause active disease in a newly infected host when latency is favoured. However, if active disease is favourable, then there is no selective pressure on the speed of progression, since the potential degree of latency of an adapted pathogen will be very close to its realised infection phenotype in the active state. In this case, the fitness cost of leaving the active state will be minimal.

We can also conclude that Condition (E.4) corresponds to a necessary (but not sufficient) condition for latency to be uniquely favoured, Condition (E.9) corresponds to a necessary (but not sufficient) for fully active infection to be uniquely favoured, and Condition (E.7) is a necessary (but not sufficient) condition for intermediate latency of degree $x = x^*$ to be uniquely favoured.

A reasonable assumption to make for a typical pathogen is that the transmission rate is a decreasing function of latency: $\beta'(\cdot) < 0$. In this case, the conditions for an internal maxima of R_0 at $x = x^*$ [Conditions (E.1)–(E.3)] can only be satisfied if $\lambda'(x^*) < 0$. Furthermore, if $\lambda''(x^*) < 0$, then $\beta''(x^*) < 0$ must also hold true. In this scenario, the necessary condition for full latency ($x = 1$) to be favoured [Condition (E.4)] will only hold true if $\lambda(1) < \lambda(0)$, while the necessary condition for partial latency ($x = x^*,\ 0 < x^* < 1$) to be favoured [Condition (E.7)] can only be satisfied if $\lambda(x^*) < \lambda(0)$.

Now we determine the conditions under which the GMR exists at phenotype coordinates which make survival possible for a pathogen. Persistence (or sustained transmission) is only possible if the GRM is greater than unity. If the GMR occurs at $(x^*,1)$, then $R_0 > 1$ when $\beta(x^*) > \lambda(x^*)$. If the GMR occurs at $(1,1)$, then $R_0 > 1$ when $\beta(1) > \lambda(1)$. Finally, if the GMR occurs at $x = 0$, then $R_0 > 1$ when $\beta(0) > \lambda(0)$.

From Eq. (C.1) it is clear that R_0 varies linearly in y. For a given value of potential latency x, the gradient of R_0 in the y direction is determined by the transmission and loss functions $\beta(\cdot)$ and

$\lambda(\cdot)$:

$$\frac{\partial R_0}{\partial y} = \frac{\lambda(0)\beta(x) - \beta(0)\lambda(x)}{a\lambda(0) + (\lambda(0) + \omega)\lambda(x)}. \tag{E.10}$$

$\partial_x R_0$ has a more complicated form:

$$\frac{\partial R_0}{\partial x} = \frac{[\lambda(0)y + \omega]\left[\beta'(x)(a\lambda(0) + (\lambda(0) + \omega)\lambda(x)) - \lambda'(x)(a\beta(0) + (\lambda(0) + \omega)\beta(x))\right]}{[a\lambda(0) + (\lambda(0) + \omega)\lambda(x)]^2}. \tag{E.11}$$

However, it is straightforward to see that for a given probability y that an infecting strain enters a latent state upon infection, the gradient of R_0 in the x direction is always steepest when $y = 1$ since

$$\frac{\partial R_0}{\partial x}(x, y) = \frac{\partial R_0}{\partial x}(x, 1)\left(\frac{\omega + y\lambda(0)}{\omega + \lambda(0)}\right). \tag{E.12}$$

Furthermore, active strains ($x = 0$) will initially incur a fitness cost if they adapt a more latent phenotype (*i.e.*, $\partial_x R_0(0, y) < 0$) when

$$\beta'(0)\lambda(0) < \lambda'(0)\beta(0).$$

However, Eq. (E.12) tells us that this cost is minimised for strains which always transmit in an active state ($y = 0$) and if $\lambda(0) \gg \omega$.

Therefore, if adopting latency properties initially comes at a cost to active strains, then those strains which are mostly causing active disease and which have very low rates of regression relative to their infection loss rate, will be able to accumulate latency properties and avoid the negative effects of selection which would otherwise significantly affect their fitness.

F. Dynamic fitness landscape

To study the evolution of tuberculosis latency, we consider two alternative possible fitness landscapes for different periods in the history of TB in human populations: 1. when *M. tuberculosis* can be considered as an emerging infectious disease with a short history of association with human hosts (landscape 1); 2. when *M. tuberculosis* can be considered as a specialised human pathogen with a long history of association with human hosts (landscape 2). We assume that the second landscape evolves from the first landscape due to evolution of the interaction between host and *M. tuberculosis* precursor that affects the ability of a host with a latent infection to recover from (or clear) the infection.

When the pathogen has a relatively short history of association with the host (landscape 1), we assume that x, the degree of latency of a latent infection, has an inverse relationship to the pathogen's growth rate, so that the host will more easily recover from a latent infection than an active infection. As the association between the host and pathogen continues, we propose that the pathogen's ability to manipulate the host immune response in the latent state and the host's ability to contain the infection evolve so that the clearance rate for latent infections begins to decrease. This continues until the host recovery rate in the latent state becomes less than that in the active state (landscape 2). In this case x becomes a measure of the degree of manipulation of the host immune response.

For our simulations, we modelled this evolution with the following functional form of the host-recovery rate:

$$\gamma(x; \eta, \epsilon) = \epsilon\left(1 + \frac{\eta}{1 + e^{-20(x-0.3)}}\right), \quad \epsilon \geq 0, \quad -1 \leq \eta \leq 1. \tag{F.1}$$

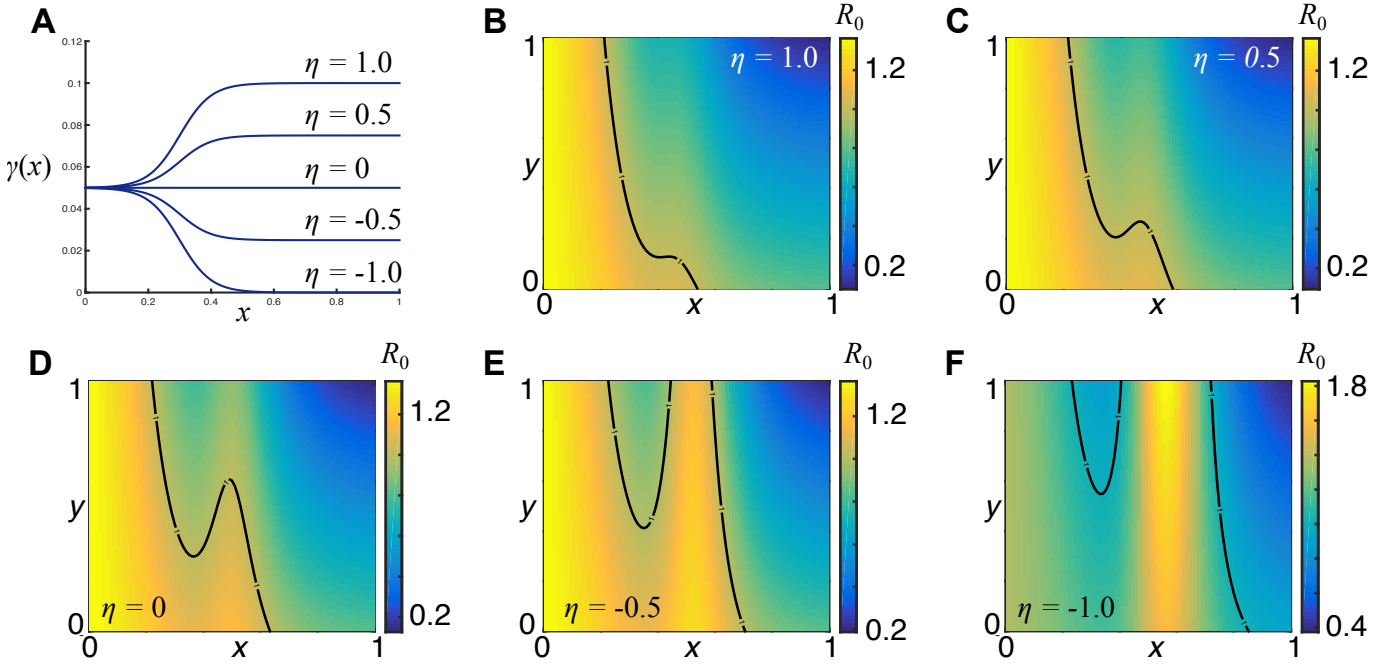

Figure S3: Fitness landscape modification due to evolution of host-pathogen interactions. Evolution is modelled as a decrease in η which modifies the shape of the host recovery rate [Eq. (F.1)] as shown in Panel A. Panels B–F display the fitness landscape for $\eta = 1, 0.5, 0, -0.5, -1$ respectively with $\epsilon = 0.05$ and the black lines indicate the contour $R_0 = 1$. If evolution of the interaction progresses far enough, active infection stops being the optimal persistence strategy for *M. tuberculosis*. Instead, an intermediate degree of latency is favoured, although a valley in the fitness landscape may interfere with active infections adopting latency properties. The forms of parameters as functions of potential latency x and other parameter values are provided in Section G.

For $\eta > 0$, $\gamma(x)$ is increasing and x is inversely related to a latent pathogen's growth rate. Evolution of the host-pathogen interaction is modelled as a decrease in η. When $\eta < 0$, $\gamma(x)$ is decreasing and x is a measure of the degree of manipulation of the host immune response by a latent infection. These ideas are illustrated in Figure S3 where we plot the evolving fitness landscape as η decreases from 1 to -1 for a given value of ϵ.

We modelled landscapes 1 and 2 using the extreme values $\eta = 1$ and $\eta = -1$, while for both periods in the history of association between *M. tuberculosis* and humans we choose a decreasing $\beta(\cdot)$ and decreasing $\theta(\cdot)$, since we expect that, in general, more latent infections will always be less transmissible and less virulent for *M. tuberculosis*.

Today, tuberculosis is considered a life-long disease. However, the *M. tuberculosis* precursor that first encountered humans likely caused only sporadic infection in its human hosts much like opportunistic environmental mycobacteria today [2]. Environmental mycobacteria tend to infect immunocompromised hosts more so than immunocompetent hosts [3]. Therefore, we assume that recovery from infection by the *M. tuberculosis* precursor was possible, and choose an ϵ with the same order of magnitude as the other epidemiological parameters. However, if we were to model the future evolution of tuberculosis we should consider $\gamma'(\cdot) < 0$ with $\epsilon \ll 1$.

G. Details of simulations

Numerical computations were performed in MATLAB. We selected a uniform discretisation on the interval $(x, y) \in [0, 1]^2$ as the phenotype domain (lattice spacing $\Delta = 10^{-2}$), and the interval $t \in [0, T]$ as the time domain (time-step length $\tau = 10^{-2}$ years). The values of all other parameters and functional forms used in the agent-based computational model and the integrodifferential equation model are listed below. Time is considered here in units of years, while all rates (β, θ, γ, μ, a and ω) have units year^{-1}, *e.g.*, $a = 0.01$ represents a reactivation rate of 0.01 infections per year.

Figure 2 and **Figure S2**. $S_0 = N - 20$, $T = 2 \times 10^3$, (a)–(b) $\beta(x) = 0.55/(1 + e^{8(x-0.3)})$, $\gamma(x) = 0.1 + 0.1/(1 + e^{-20(x-0.3)})$, $\theta(x) = 0.02 + 0.3/(1 + e^{20(x-0.4)})$, $\omega = 0.3$, $a = 0.01$, $\mu = 1$, $N = 1000$; (c)–(d) $\beta(x) = 0.2/(1 + e^{10(x-0.6)})$, $\gamma(x) = 0.25/(1 + e^{-5(x-0.9)})$, $\theta(x) = 0.02 + 0.3/(1 + e^{7(x-0.1)})$, $\omega = 0.2$, $a = 0.01$, $\mu = 3/\sqrt{10}$, $N = 100$; (e)–(f) $\beta(x) = 0.05 + 0.21/(1 + e^{2(x-0.95)})$, $\gamma(x) = 0.05$, $\theta(x) = 0.02 + 0.2/(1 + e^{7(x-0.6)})$, $\omega = 0.2$, $a = 0.01$, $\mu = 1$, $N = 200$; (b) $\bar{\gamma}(x) = 0.1/(1 + e^{20(x-0.3)})$ (grey dash-dot line).

Figure 3. $a = 0.01$, $\mu = 1$, $N = 10^5$, $S_0 = N - 20$, $T = 5 \times 10^3$, $\beta(x) = 0.55/(1 + e^{8(x-0.3)})$, $\gamma(x) = 0.1/(1 + e^{20(x-0.3)})$, $\theta(x) = 0.02 + 0.3/(1 + e^{20(x-0.4)})$. (a) $\omega = 0.3$; (b) $\omega = 0.05$.

Figure S3. $\beta(x) = 0.55/(1 + e^{8(x-0.3)})$, $\gamma(x) = 0.05(1 + \eta/(1 + e^{-20(x-0.3)}))$, $\theta(x) = 0.02 + 0.3/(1 + e^{20(x-0.4)})$, $a = 0.01$, $\omega = 0.3$, (a) $\eta \in \{1, 0.5, 0, -0.5, -1\}$; (b) $\eta = 1$; (c) $\eta = 0.5$; (d) $\eta = 0$; (e) $\eta = -0.5$; (f) $\eta = -1$.

Movie S1. $a = 0.01$, $\mu = 1$, $N = 10^5$, $S_0 = N - 20$, $T = 5 \times 10^3$, $\beta(x) = 0.55/(1 + e^{8(x-0.3)})$, $\gamma(x) = 0.1/(1 + e^{20(x-0.3)})$, $\theta(x) = 0.02 + 0.3/(1 + e^{20(x-0.4)})$, $\omega = 0.05$.

Table S1: Values of model parameters used in the simulations of the emergence of latency shown in Figure 3.

Parameter	Symbol	Value	Source
Mutation rate	μ	1 per year[¶]	[4]
Activation rate	a	0.01 per year	[5]
Regression rate	ω	0.30 per year[†]	[5, 6, 7]
Host death rate with active infection	$\theta(0)$	0.32 per year[*]	[8]
Host natural death rate	$\theta(1)$	0.02 per year[‡,*]	[5, 7]
Host transmission rate in active state	$\beta(0)$	0.50 per year[*]	chosen so $R_0(x, y) > 1$ for $x = 0$
Host transmission rate in latent state	$\beta(1)$	0 per year[*]	assume no transmission from latent hosts
Host recovery rate with active infection	$\gamma(0)$	0.10 per year[*]	[9]
Host recovery rate with latent infection (short history of association)	$\gamma(1)$	0.20 per year[*]	
Host recovery rate with latent infection (long history of association)	$\gamma(1)$	0 per year[*]	assume life-long infection for latent hosts
Maximum susceptible host population size[§]	N	10^5	[10]
Phenotype length scale	Δ	0.01	arbitrary choice

[¶] Roughly the rate of single nucleotide polymorphisms per genome

[†] $\omega = 0.05$ per year for the case where latency emerges

[‡] Same as latently-infected host death rate

[*] These values are rounded for display, all other values are exact.

[§] Calculated as 10 × effective size of hunter-gatherer populations

H. Caption for electronic supplementary material, movie S1

One simulation of the model showing how active pathogens can cross a fitness valley to reach a higher peak at latency by cryptically accumulating costly latency properties. Here, the population of infections is superimposed over the density plot of the fitness landscape R_0. A red dot represents one active infection, a blue represents one latent infection and infection phenotypes are indicated by their positions on the landscape.

References

[1] Heffernan, J., Smith, R. & Wahl, L. 2005 Perspectives on the basic reproductive ratio. *J R Soc Interface.* **2**, 281–293.

[2] Simpson, G. L., Raffin, T. A. & Remington, J. S. 1982 Association of prior nocardiosis and subsequent occurrence of nontuberculous mycobacteriosis in a defined, immunosuppressed population. *J Infect Dis.* **146**, 211–219.

[3] Galagan, J. E. 2014 Genomic insights into tuberculosis. *Nat Rev Genet.* **15**, 307–320.

[4] Walker, T. M., Ip, C. L., Harrell, R. H., Evans, J. T., Kapatai, G., Dedicoat, M. J., Eyre, D. W., Wilson, D. J., Hawkey, P. M., Crook, D. W. *et al.* 2013 Whole-genome sequencing to delineate *Mycobacterium tuberculosis* outbreaks: a retrospective observational study. *Lancet Infect Dis.* **13**, 137–146.

[5] Zheng, N., Whalen, C. C. & Handel, A. 2014 Modeling the potential impact of host population survival on the evolution of *M. tuberculosis* latency. *PLoS ONE.* **9**, e105721.

[6] Dye, C. & Espinal, M. A. 2001 Will tuberculosis become resistant to all antibiotics? *Proc R Soc Lond B.* **268**, 45–52.

[7] Basu, S. & Galvani, A. P. 2009 The evolution of tuberculosis virulence. *Bull Math Biol.* **71**, 1073–1088.

[8] Tiemersma, E. W., van der Werf, M. J., Borgdorff, M. W., Williams, B. G. & Nagelkerke, N. J. 2011 Natural history of tuberculosis: duration and fatality of untreated pulmonary tuberculosis in HIV negative patients: a systematic review. *PLoS ONE.* **6**, e17601.

[9] Blower, S. M., Mclean, A. R., Porco, T. C., Small, P. M., Hopewell, P. C., Sanchez, M. A. & Moss, A. R. 1995 The intrinsic transmission dynamics of tuberculosis epidemics. *Nat Med.* **1**, 815–821.

[10] Kim, H. L., Ratan, A., Perry, G. H., Montenegro, A., Miller, W. & Schuster, S. C. 2014 Khoisan hunter-gatherers have been the largest population throughout most of modern-human demographic history. *Nat Commun.* **5**, 5692.